

Removal of coherent noise from electroseismic data

Seth Haines and Antoine Guitton¹

ABSTRACT

The electroseismic method offers the possibility of imaging thin (much smaller than the seismic wavelength) layers in the subsurface. Removal of coherent source-generated noise is an essential step in the processing of electroseismic data. We present a signal-noise separation technique that begins with the determination of signal and noise prediction error filters (PEF's) from windows of the original data and uses these PEF's in an iterative inversion for signal and noise models. The noise residual is weighted during the inversion to prevent the comparatively weaker (by about two orders of magnitude) signal from being obscured by the coherent noise. Application of this processing sequence to real data, in which synthetic signal arrivals are obscured, demonstrates the effectiveness of the technique.

INTRODUCTION

A seismic wave traveling through a fluid-saturated porous material carries with it a charge separation created by the pressure-induced flow of pore fluid. The pore fluid carries a small (but not inconsequential) amount of electric charge relative to the adjacent grains due to the electric double layer (Shaw, 1992) that exists at the grain-fluid boundary. Thus, an electric field (Figure 1) is co-located with a compressional (P) wave propagating through such a material (Pride, 1994). We refer to this field as the “coseismic” field.

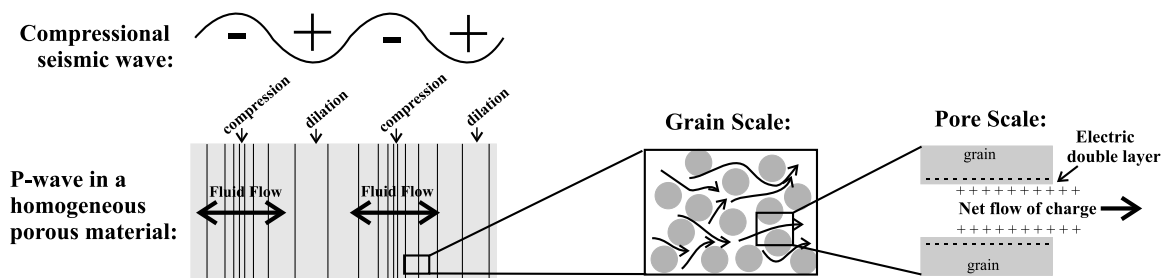
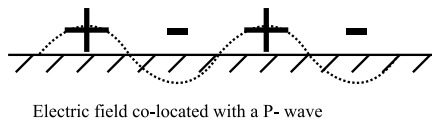


Figure 1: Electroesismic phenomena depend on the charge separation created by streaming currents that flow in response to the pressure gradient of a seismic wave. The electric double layer is responsible for streaming currents at the grain scale. [shaines1-esbasics] [NR]

¹email: shaines@pangea.stanford.edu, antoine@sep.stanford.edu

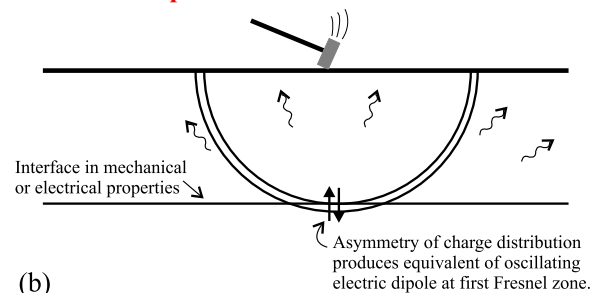
The second aspect of the electroseismic response occurs when the P-wave encounters an interface in material properties (elastic, chemical, flow-related, etc). The charge separation in the wave (Figure 2) is disturbed, causing asymmetry and results in what can be approximated as an oscillating electric dipole at the first Fresnel zone (Haartsen and Pride, 1997). Essentially, the entire region of the first Fresnel zone acts as a disk of vertical electric dipoles. Thus, the resulting electric field is that of a dipole, with opposite polarity on opposite sides of the source point and amplitudes diminishing as $1/z^3$ (where z is the depth to the interface). This field (Figure 2b), called the “interface response,” can be measured almost immediately at the Earth’s surface since the travel-time of electromagnetic radiation is negligible compared with seismic travel-times ($V_{EM} \gg V_P$).

“Coseismic Field”



(a)

“Interface Response”



(b)

Figure 2: Two types of electroseismic effects that can be measured with electrode dipoles at the Earth’s surface: (a) the coseismic field of a P-wave at the surface (represented here by the charge accumulations “+” and “-”), and (b) the interface response created when the P-wave hits an interface at depth. [shaines1-2effects](#) [NR]

Both effects can be measured in the field using a standard seismograph equipped with electrode dipoles instead of geophones (Haines et al., 2001; Garambois and Dietrichz, 2001; Thompson and Gist, 1993). The coseismic field traveling with the seismic wave is not particularly interesting since it contains information only about the properties of the surface of the Earth. The interface response, on the other hand, can provide new information about the subsurface. In particular, the interface response is created even for very thin layers, such as a thin fracture zone in otherwise solid rock, or a thin impermeable layer in an aquifer or reservoir. Haines et al. (2001) show that the interface response from a saturated permeable layer 0.6-m thick can be reliably observed. Numerical simulations show that the interface response from a 1-cm embedded impermeable layer is significantly greater than that from an interface between two layers (Stephane Garambois, personal communication 2001). Thus the electroseismic method promises to provide valuable information about important subsurface targets that can not be imaged using other geophysical methods, including information about the location of changes in flow properties. It is our goal to develop a protocol that can be used to reliably and repeatably acquire, process, and interpret electroseismic data.

Unfortunately, electroseismic data collected with a geometry similar to conventional surface seismic data is comprised of both the interface response from subsurface layers and unwanted coseismic energy recorded simultaneously. Coseismic energy, roughly 100 times the amplitude of the interface response, therefore represents a formidable form of coherent

source-generated noise. The removal of this noise is essential to the utility of the electroseismic method, so the development of an effective data processing approach is an important step toward this goal. The use of transforms (e.g., f-k filtering) has proven ineffective on available data due to the overpowering amplitude of the coseismic noise, and the fact that the top of the coseismic energy hyperbola tends to be smeared across the record during the inverse transform. It is essential that all horizontal energy remaining in the record after processing be only from the interface response. Each shot record eventually will be stacked to produce a single trace corresponding with the subsurface region beneath the shot point. Thus, smeared coseismic energy would be very detrimental to the final stack in much the way that inclusion of ground roll or refractions negatively impacts a stacked seismic reflection section. In addition, the smearing of energy represents a loss of amplitude information and the retention of relative amplitudes is desired.

We present a data processing strategy that separates the signal of interest from the stronger coherent noise. This strategy incorporates the coherent noise subtraction approach described by Guitton (2001) while building on the use of PEF's described by Claerbout and Fomel (2001). An important feature of our approach is its preservation of the signal amplitude made possible by our use of iterative inversion. We also present other data processing options and discuss the work remaining to be completed before the electroseismic method can be considered a reliable tool.

EXPERIMENTAL DATA

Haines et al. (2001) present electroseismic experimental methods designed to record the coseismic field and the interface response separately. By imaging a vertical interface with the source and receivers on opposite sides of the target (Figure 3), they record the interface response before the coseismic energy (Figure 4). The target is a trench $\sim 0.6\text{m}$ wide, $\sim 2\text{m}$ deep, and $\sim 18\text{m}$ long, lined with plastic, and filled with wet sand.

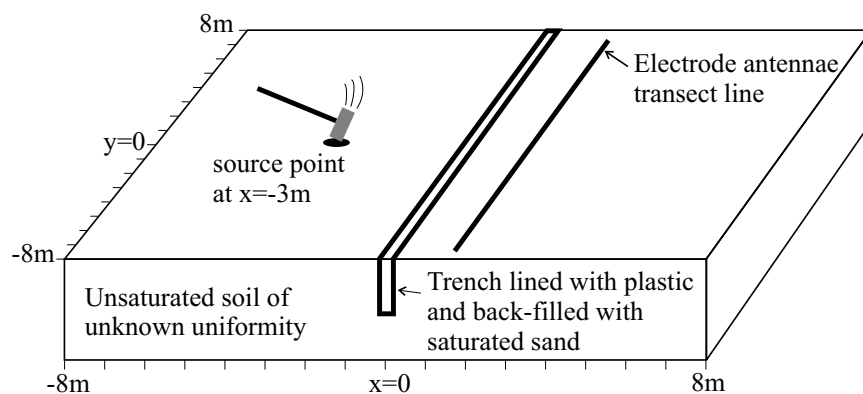
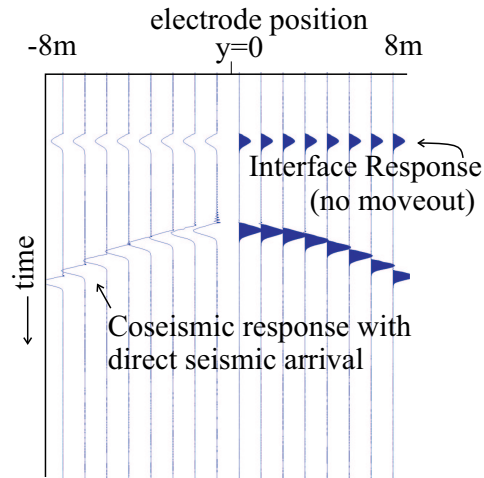


Figure 3: Layout of field site. Note that source and receivers are on opposite sides of the target so that the seismic wave creates the interface response at the trench before reaching the electrodes and being recorded as the coseismic energy. [shaines1-layout](#) [NR]

Figure 4: Generalized data, showing interface response arriving before coseismic energy. Note reversed polarity on opposite sides of shot point. (For simplicity, relative amplitudes are NOT correct.)

shaines1-gen_data [NR]



Approximately 80 shot records have been recorded at this site with various shot and receiver geometries. Shot gathers are generally stacks of 50 to 100 strikes of a 12 lb sledgehammer on a metal plate located 1 to 4 meters from one side of the trench. Recording geometries include 24 electrode dipoles (~ 1 meter wide) at ~ 0.7 m spacing located 1 to 4 meters from the other side of the trench. The interface response is recognizable before the coseismic arrival on every record, with varying clarity and strength. Arrival times and simple amplitude modeling confirm that the observed signal is indeed the interface response. Because the interface response shows virtually no moveout, and because it has reversed polarity on opposite sides of the shot point, it can be visually differentiated from the coseismic arrival and background electrical noise. These data, with the two effects recorded separately, provide a unique opportunity for development of a processing sequence to enhance the interface response and remove the coseismic signal.

SIGNAL-NOISE SEPARATION

Electroseismic data (\mathbf{d}) can be thought of as the sum of three distinct elements- the interface response signal (\mathbf{s}), the coseismic noise (\mathbf{n}), and background electrical noise (\mathbf{n}_{bg}):

$$\mathbf{d} = \mathbf{s} + \mathbf{n} + \mathbf{n}_{bg}. \quad (1)$$

In order to separate the interface response from the coseismic noise, we implement a signal-noise separation technique using separate PEF's \mathbf{A}_s and \mathbf{A}_n for the signal and noise respectively. Because much of \mathbf{n}_{bg} is not readily predictable, it cannot be modeled with a PEF. We minimize \mathbf{n}_{bg} with pre-processing.

Pre-processing

Raw electroseismic data is dominated by energy from the power grid at harmonics of 60 Hz (Figure 5a). We remove this noise using the sinusoid subtraction technique of Butler and

Russell (1993) for all harmonics of 60 Hz up to the Nyquist frequency. Coseismic energy is generally lower in frequency than the interface response due to a greater distance of travel as a seismic wave, so we use a low-cut filter to begin the process of noise removal. We also employ a high-cut filter to minimize background noise that can obscure weaker arrivals (Figure 5b).

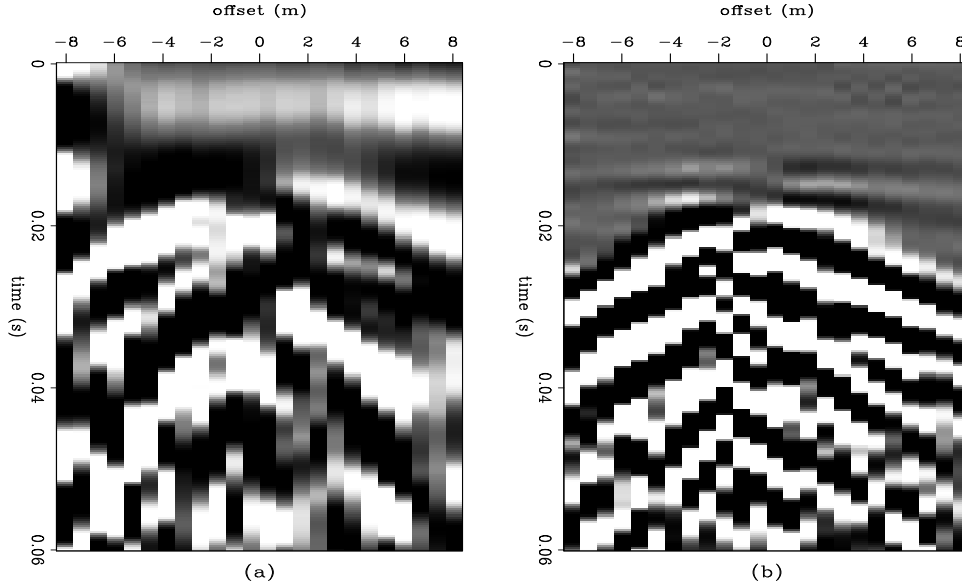


Figure 5: (a) Raw data. (b) Same file, with 60 Hz energy removed and bandpass filter (120-500 Hz) applied. Note horizontal interface response event at 0.015 seconds. [shaines1-basic526](#) [ER,M]

Processing approach

The PEF's \mathbf{A}_s and \mathbf{A}_n are determined from windows of the data file that are particularly representative of each. It is essential to have good design windows for the two PEF's, representative of the two components \mathbf{s} and \mathbf{n} . We determine only one PEF for the entire data file, thus assuming (perhaps unwisely) stationarity. Using the PEF's \mathbf{A}_s and \mathbf{A}_n , we perform an iterative inversion to determine signal and noise models \mathbf{m}_s and \mathbf{m}_n with the fitting goal (Guitton, 2001):

$$\mathbf{0} \approx \mathbf{L}_s \mathbf{m}_s + \epsilon \mathbf{L}_n \mathbf{m}_n - \mathbf{d}, \quad (2)$$

where

$$\mathbf{L}_s = \mathbf{A}_s^{-1} \text{ and } \mathbf{L}_n = \mathbf{A}_n^{-1}.$$

We solve the following least squares inverse formulation of equation (2):

$$\begin{pmatrix} \hat{\mathbf{m}}_n \\ \hat{\mathbf{m}}_s \end{pmatrix} = \begin{pmatrix} \epsilon^{-1} (\mathbf{L}'_n \overline{\mathbf{R}}_s \mathbf{L}_n)^{-1} \mathbf{L}'_n \overline{\mathbf{R}}_s \\ (\mathbf{L}'_s \overline{\mathbf{R}}_n \mathbf{L}_s)^{-1} \mathbf{L}'_s \overline{\mathbf{R}}_n \end{pmatrix} \mathbf{d},$$

with

$$\begin{aligned}\overline{\mathbf{R}}_s &= \mathbf{I} - \mathbf{L}_s(\mathbf{L}'_s\mathbf{L}_s)^{-1}\mathbf{L}'_s, \\ \overline{\mathbf{R}}_n &= \mathbf{I} - \mathbf{L}_n(\mathbf{L}'_n\mathbf{L}_n)^{-1}\mathbf{L}'_n,\end{aligned}\quad (3)$$

as defined by Guitton et al. (2001). The estimated noise $\hat{\mathbf{n}}$ and signal $\hat{\mathbf{s}}$ are then computed by

$$\begin{aligned}\hat{\mathbf{n}} &= \mathbf{L}_n\hat{\mathbf{m}}_n, \\ \hat{\mathbf{s}} &= \mathbf{L}_s\hat{\mathbf{m}}_s.\end{aligned}\quad (4)$$

The weighting factor ϵ in equation () is crucial to this process. As $\epsilon \rightarrow 1$, $\mathbf{L}_s\hat{\mathbf{m}}_s$ is given too little importance in the inversion relative to $\mathbf{L}_n\hat{\mathbf{m}}_n$ and $\hat{\mathbf{m}}_s$ is polluted with large amounts of noise. Physically, ϵ represents the magnitude difference between the two distinct physical processes that make up the electroseismic response. These two processes are: the generation of electromagnetic energy by an oscillating electric dipole (observed from a distance, called the interface response), and the generation of an electric field within a passing seismic wave (measured directly, called the coseismic field).

Because the fitting goal does not include a term for \mathbf{n}_{bg} , any background noise remaining in the data after pre-processing simply falls into the residual. This is necessary because \mathbf{n}_{bg} is difficult to model, and acceptable because $\|\mathbf{n}_{bg}\| < \|\mathbf{s}\| \ll \|\mathbf{n}\|$. Convolution of the PEF's with the data is accomplished using the helix of Claerbout (1998).

To summarize the processing sequence:

1. Frequency filtering and 60 Hz removal
2. Second time derivative and other preprocessing steps described later
3. Determine \mathbf{A}_s and \mathbf{A}_n from windows of data file
4. Iteratively solve the inverse problem of equation (). Output $\hat{\mathbf{s}} = \mathbf{L}_s\hat{\mathbf{m}}_s$.

Implementing the data processing sequence

Because we determine only one set of PEF's for a given processing effort, we improve the ability of the PEF's to model their respective parts of the data by processing only half the traces at one time (in this case, the positive offsets). Therefore, the noise is more easily modeled since all coseismic energy dips in the same direction. We include the three nearest negative-offset traces so that the final result (after "losing" traces to convolution with PEF's) includes all of the positive offset traces.

Data processing begins with the selection of suitable windows for determination of PEF's \mathbf{A}_s and \mathbf{A}_n . With these windows chosen, we can test different parameters for the rest of the processing, namely the sizes of the two PEF's, the value of the weighting factor ϵ , and the number of iterations for the inversion.

Because the signal of interest is horizontal, it is logical to use a signal PEF \mathbf{A}_s that has only one element in the vertical direction. This assumption is confirmed by experimentation, as taller PEF's are less effective at modeling non-horizontal energy. We find that a width of 4 is a fair trade-off between the better resolution of a wider PEF and the smaller number of traces lost to convolution afforded by a narrower PEF. The size of the noise PEF \mathbf{A}_n is more arbitrary, but we find that dimension 4x3 yields satisfactory results.

ϵ is best determined experimentally, though the development of a more rigorous approach would improve the versatility of the processing sequence. Interestingly, a broad range of ϵ values results in essentially the same final result. We find $\epsilon = 0.01$ to be a reasonable value for the data shown here. Finding a reasonable criteria to define the end of the iterative inversion process is another aspect of this processing sequence that deserves more attention. We have simply stopped the inversion after 350 iterations.

Testing the processing sequence

Data collected by Haines et al. (2001) was designed to record the interface response and coseismic energy separately as a test data set for processing. However, these files lack any additional interface response events after the onset of coseismic energy (Figure 6a). In an electroseismic data set collected with a standard geometry, we would be looking for interface response events within the coseismic energy. For that reason, we followed the example of Brown and Clapp (2000) and constructed a test data file by windowing out (Figure 6b) the interface response from a record (Figure 6a) using a \sin^2 taper in the time direction and adding it to the original file within the coseismic energy. We did this twice (Figure 6c), adding the synthetic arrival at two different times in the record. The resulting record (Figure 6d) appears essentially identical to the original file, but contains two interface response events hidden within to test our methodology.

Using the PEF design windows shown (Figure 7b and c), and the parameters mentioned above, we solve the inverse problem (equation). Figure 7d shows \hat{s} , our best estimate of s , the component of the data that is made up of the interface response energy. The two added interface response events are evident, as is the original interface response. Unfortunately, a considerable amount of dipping coseismic energy still remains between 0.025 and 0.04 seconds, and the added event below 0.06 seconds is somewhat weak. Despite these shortcomings, the final result (Figure 7d) is considerably better than the original data file (7a).

Additional pre-processing steps

The results shown in Figure 7 demonstrate that the basic algorithm can be effective. However, the low amplitude of the added interface response events relative to the remaining coseismic noise suggests that additional pre-processing steps should be explored in order to improve the final result. In this vein, we tested the use of a second time derivative as a means of balancing the amplitudes of the interface response relative to the coseismic energy. This spectral balancing enhances the generally higher-frequency interface response. This step sharpens the image

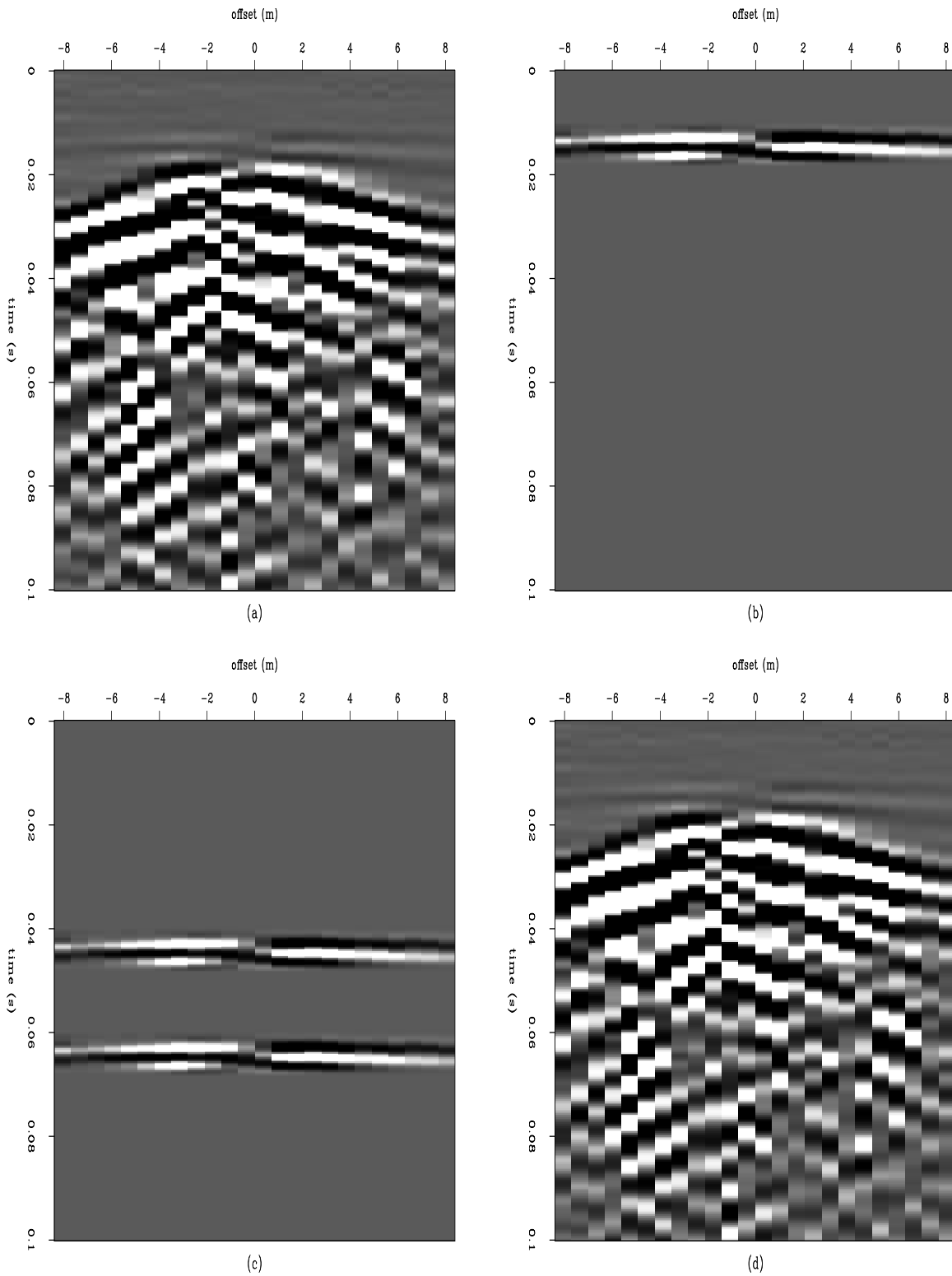


Figure 6: (a) Data file. (b) Interface response (IR) from (a), windowed with \sin^2 taper. (c) Two IR events to be added to data. (d) Test data- starting data plus two added events. shaines1-fake
 [ER,M]

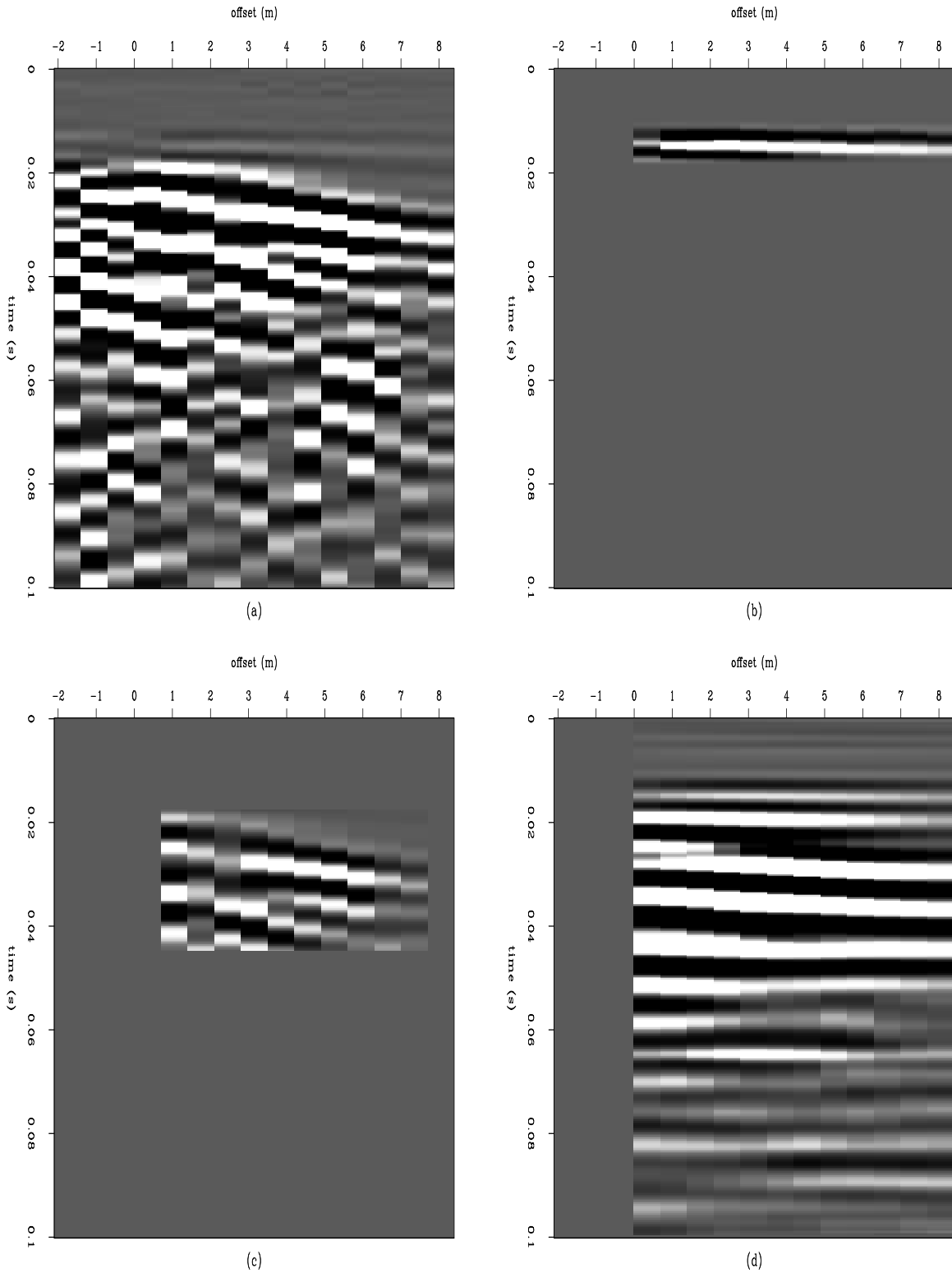


Figure 7: (a) Data file (windowed version of file in 6d). (b) Window to be used for determination of signal PEF \mathbf{A}_s . (c) Window used for determination of noise PEF \mathbf{A}_n . (d) Output of processing, $\mathbf{L}_s \hat{\mathbf{m}}_s$. Note that added horizontal events 0.045 s and 0.065 s are visible.

shaines1-nice [ER,M]

(Figure 8a), and improves the ability of the PEF to precisely locate the signal amidst the noise. Applying the same processing steps as used for Figure 7 and using the same parameters, we find that the end result (Figure 8d) is markedly improved over Figure 7d, with greater clarity of the added events.

Still present is the dipping coseismic energy between 0.025 and 0.04 seconds. Because this energy is so strong, and so close to horizontal, it leaks through the PEF, corrupting a portion of the record. This problem is the focus of on-going investigation and is being addressed with waveform separation.

Waveform separation is a standard technique in VSP and cross-well seismic processing, used to remove high-amplitude early arrivals in records by capitalizing on the different move-outs of different arrivals. We employ the method as follows: (1) picks are manually made along the arrival targeted for removal, (2) the gather is moved out such that the arrival (as defined by the picks) is horizontal and then stacked, and (3) the resulting trace is normalized by the number of traces in the gather and then subtracted from each of the moved-out traces. (4) After the subtraction, the gather is moved back to its original alignment. By repeating this process, it is possible to remove more than one coherent arrival from the record. Figure 9 shows a series of images as various arrivals are removed from the record (9a). Figure 9d shows the result after three iterations through the process, and shows that although the process has effectively removed much of the energy of the strong coseismic first arrivals, it has also partially removed the interface response (0.01 to 0.02 seconds). This is a result of the chance line-up of waveforms during the second iteration. We chose to use the data shown in Figure 9c for the PEF processing sequence.

We apply the second derivative after waveform separation since it has proven successful. Because the coherence of the coseismic noise has been disturbed by the waveform separation technique, we opt to determine the PEF's A_s and A_n with the data shown in the windows of Figure 8b and c. The starting datafile (after waveform separation and second derivative) is shown in Figure 10a, with the final result in Figure 10b. Here we see that the clarity of the added events is improved, but that some of the coseismic energy remains. In this case, the remaining coseismic energy is closer to horizontal than that in Figure 8d. Thus, if we were to stack this gather, the resulting trace would definitely include unwanted coseismic energy. We continue to pursue solutions to this problem.

SUMMARY

At this time, our preferred processing sequence is:

1. Remove 60 Hz energy
2. Bandpass filter
3. Waveform separation
4. Second time derivative

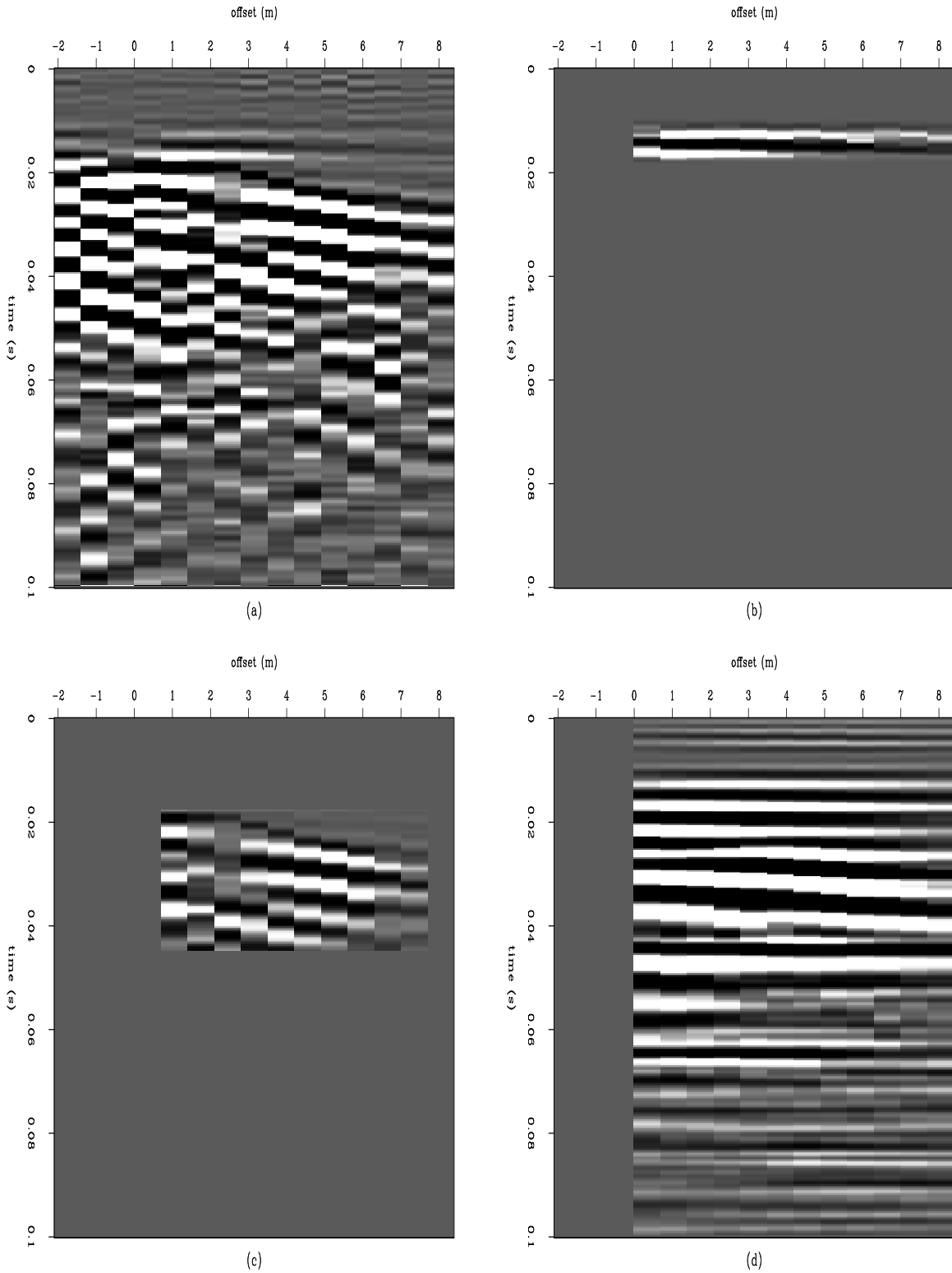


Figure 8: (a) Data file (second time derivative of file in 7a). (b) Window for determination of signal PEF \mathbf{A}_s . (c) Window for determination of noise PEF \mathbf{A}_n . (d) Output of processing, $\mathbf{L}_s \hat{\mathbf{m}}_s$. Note that added horizontal events 0.045 s and 0.065 s are visible. shaines1-nice2D
[ER,M]

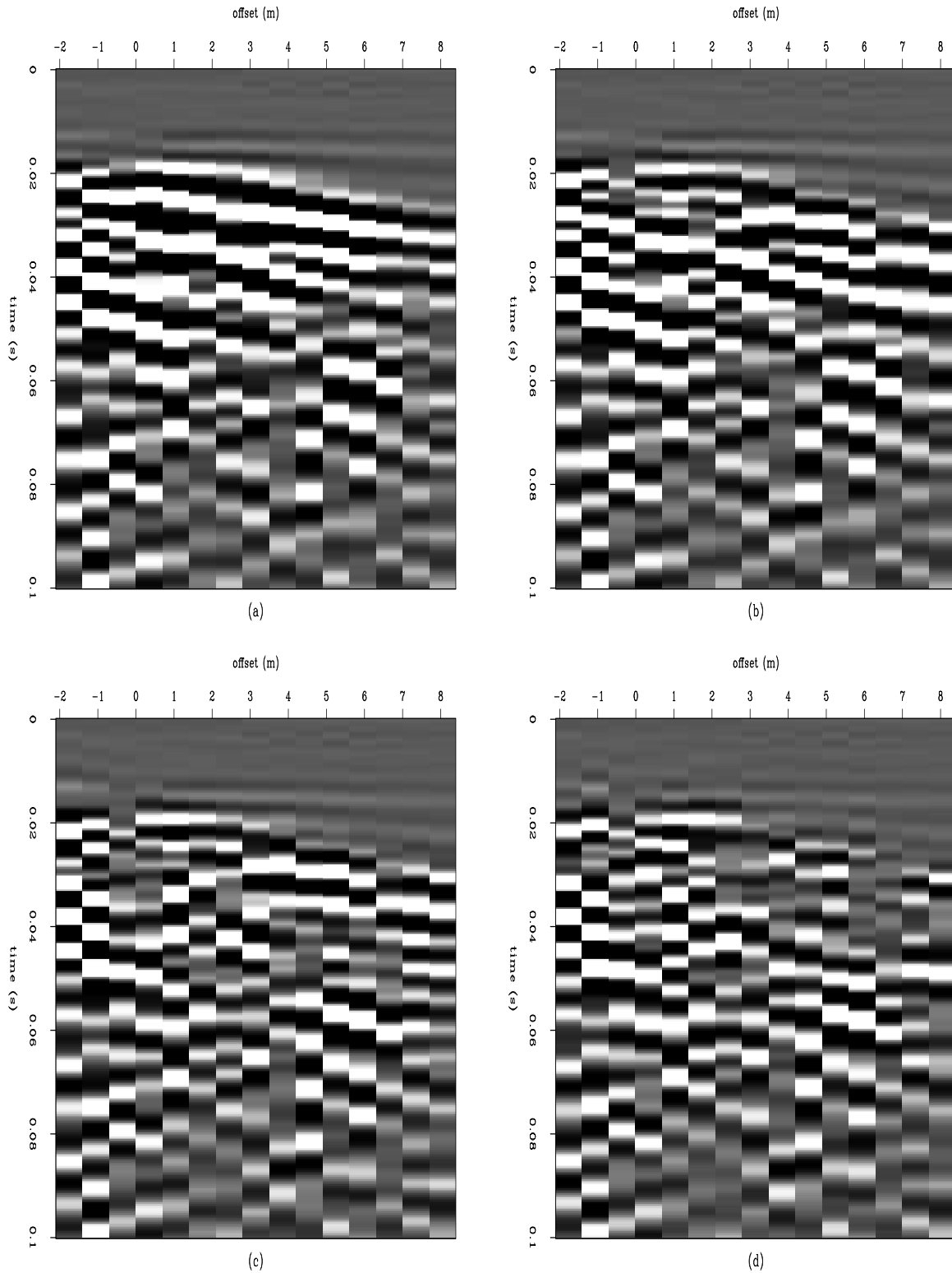


Figure 9: (a) Data file (same as 7a). (b) Result after one iteration through waveform separation process. (c) Result after second iteration. This is the file that we use in the PEF processing sequence. (d) Result after three iterations through the waveform separation process. Note that the interface response (0.01 to 0.02 seconds) event has been partially removed.

`shaines1-xwell` [ER,M]

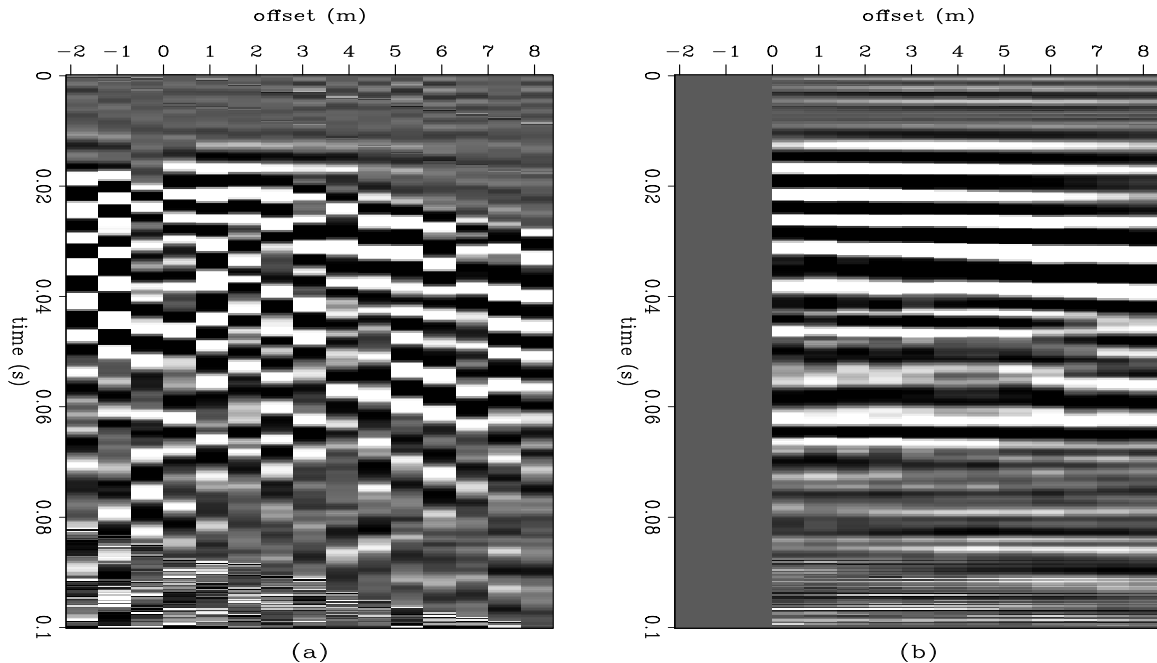


Figure 10: (a) Data file (Second derivative applied to data from Figure 9c). (b) Result after PEF processing sequence. Note that added horizontal events 0.045 s and 0.065 s are clearly visible. `shaines1-nicexwell` [ER,M]

5. Specify windows for determination of signal and noise PEF's
6. Weighted inversion for signal and noise models. Output is $\hat{\mathbf{s}} (= \mathbf{L}_s \hat{\mathbf{m}}_s \approx \mathbf{s})$.

DISCUSSION

The processing sequence presented here is shown to be effective in separating the electroseismic interface response from the much stronger coseismic noise for the artificial example used. This is interesting both as an example of signal-noise separation in a case with very low signal-to-noise ratio and also as an important step toward proving the utility of the electroseismic method. However, the results we present are unrealistic in several important ways. Most importantly, the interface response events that we separate from the noise are essentially synthetic, and undoubtedly have different amplitude and frequency patterns than real arrivals from subsurface layers. We can attempt to make the inserted arrivals more realistic by stretching and scaling them before addition, but no synthetic record can really replace real data.

Thus the next logical step in this project is to collect a more realistic electroseismic data set at a location that is thoroughly-characterized. It is important that the characterization include wells, because the method promises to image layers that are invisible to existing surface methods. An ideal survey would take place at a test site with relatively simple subsurface, but with a few thin layers (fractures, clay lenses, etc) to be targeted. The use of a vibratory

source or a high-intensity explosive source would vastly ease the recognition of the signal amidst background noise, and adding more recording channels would tremendously improve data quality and the output of data processing efforts.

A greater number of traces per shot gather will permit refinement of the processing scheme. The use of non-stationary PEF's may prove effective, since the nature of the coseismic energy clearly varies within the shot record. The use of a gap in the noise PEF may be an improvement, as it could prevent the PEF from being dominated by energy corresponding with infinite slope due to the spiky appearance of the coseismic data. In addition, a larger number of traces would improve the probability of success of transform-based methods such as f-k filtering and slant-stack filtering.

Our data processing goal is to develop a sequence that can be applied to field data in as close to an automatic manner as possible (fewer manual steps). This could include the development of generic signal and noise PEF's that would function on any data, and would not require the determination of these PEF's on windows of each data file. This would improve the processing of noisy data files (where such windows would be hard to define), and would speed the processing of data from larger-scale surveys. The results presented here suggest that this goal can be attained within a reasonable period of time, given a suitable data set for testing. The results of Haines et al. (2001) demonstrate that such a data set can be collected in the proper setting with the necessary equipment. Thus, depending on circumstances, the electroseismic method could soon begin to provide useful new subsurface information in geophysical exploration.

ACKNOWLEDGMENTS

We are grateful to Simon Klemperer for general field guidance, to Jerry Harris for suggesting the waveform separation technique and other technical tid-bits, and to Steve Pride for the field experiment design and all-around electroseismic instruction. Thanks to Jon Claerbout for suggesting the use of PEF's and other invaluable processing advice; and to all members of SEP, but particularly Brad Artman, Morgan Brown, and Bob Clapp for help getting up-to-speed on the SEP computer system, and for help with coding. Also, the data presented here would not exist without the effort of those who swung the hammer: Steve Pride, Nick Martin, Jonathan Franklin, Jordan Muller, T.J. Kiczenski and Stephan Bergbauer. Jim and Carolyn Pride graciously provided the field site, four dumptrucks full of sand, and some of their outstanding wine. Art Thompson provided some essential electronics, along with important input on data collection. Funding has been provided by the Stanford School of Earth Sciences McGee Fund, the AAPG student research grants, and by the GSA student research grants.

REFERENCES

- Brown, M., and Clapp, R., 2000, T-x domain, pattern-based ground-roll removal: 70th Ann. Internat. Mtg, Soc. Expl. Geophys., Expanded Abstracts, 2103–2106.

- Butler, K. E., and Russell, R. D., 1993, Subtraction of powerline harmonics from geophysical records (short note): *Geophysics*, **58**, no. 06, 898–903.
- Claerbout, J. F., and Fomel, S., 2001, *Geophysical Estimation by Example*: http://sepwww.stanford.edu/sep/prof/gee/toc_html/index.html.
- Claerbout, J., 1998, Multidimensional recursive filters via a helix: *Geophysics*, **63**, no. 05, 1532–1541.
- Garambois, S., and Dietrichz, M., 2001, Seismoelectric wave conversions in porous media: Field measurements and transfer function analysis: *Geophysics*, **66**, no. 5, 1417–1430.
- Guitton, A., Brown, M., Rickett, J., and Clapp, R., 2001, A pattern-based technique for ground-roll and multiple attenuation: *SEP*–**108**, 249–274.
- Guitton, A., 2001, Coherent noise attenuation: A synthetic and field example: *SEP*–**108**, 225–248.
- Haartsen, M. W., and Pride, S. R., 1997, Electrostatic waves from point sources in layered media: *J. Geophys. Res.*, **102**, no. B11, 24745–24769.
- Haines, S., Pride, S., and Klemperer, S., 2001, Development of experimental methods in electrostatic research, with application to aquifer characterization: *Eos Trans. AGU*, **82**, no. 47, Abstract GP22A–0268.
- Pride, S., 1994, Governing equations for the coupled electromagnetics and acoustics of porous media: *Physical Review B*, **50**, no. 21, 15678–15696.
- Shaw, D., 1992, *Introduction to colloid and surface chemistry*: Butterworths, 4th edition.
- Thompson, A. H., and Gist, G. A., 1993, Geophysical applications of electrokinetic conversion: *The Leading Edge*, **12**, no. 12, 1169–1173.

